Vietnam Journal of Marine Science and Technology 2024, 24(4) 349–362

Vietnam Academy of Science and Technology

Vietnam Journal of Marine Science and Technology

journal homepage: vjs.ac.vn/index.php/jmst

Application the Mike 3 model to simulate the turtibity dispersion due to sediment dumping activities in Nghi Son Port, Thanh Hoa Province

Nguyen Hong Lan*, Vu Van Lan

Hanoi University of Natural resources and Environment, Hanoi, Vietnam

Received: 21 April 2024; Accepted: 14 June 2024

ABSTRACT

The study applied the Mike 3 hydrodynamic model to simulate the turbidity propagation from sediment mud deposition activities at sea in the Nghi Son port area, Thanh Hoa province. The research results show that during the northeast monsoon period, the sediment mud concentration field is distributed southward from the deposition area, with sediment mud concentrations ranging from 0.01 kg/m³ to 0.4 kg/m³ within an influence radius of approximately 2.5 km. During the southwest monsoon period, the turbidity concentration distribution expands northward from the deposition area due to the influence of wind and currents during this season. The northern area of Nghi Son port is affected by the dispersion of turbidity concentrations below 0.04 kg/m³. The area surrounding Hon Me island has sediment mud concentrations ranging from 0.015 kg/m³ to 0.025 kg/m³. The turbidity concentration distribution with depth ranges from 0.01 kg/m³ to 0.4 kg/m³ and is primarily located at the seafloor depths ranging from -14 m to -18 m. The turbidity concentration gradually decreases towards the water surface. The turbidity concentration in the upper water layer is relatively low, ranging from 0.01 kg/m³ to 0.08 kg/m³, with depths from 0 to -5 m.

Keyword: Mike 3, turbidity, environment, hydrodynamic, port, dumping, dispersion.

*Corresponding author at: Ha Noi University of Natural resources and Environment, Hanoi, Vietnam. *E-mail addresses*: nhlan@hunre.edu.vn

https://doi.org/10.15625/1859-3097/22043

ISSN 1859-3097; e-ISSN 2815-5904/

INTRODUCTION

The East Vietnam Sea lies on vital maritime routes connecting the Pacific and Indian Oceans, Europe and Asia, and the Middle East and Asia. It is one of the top ten busiest maritime routes globally. It ranks second in maritime traffic congestion (after the Mediterranean Sea). Therefore, Vietnam is has significant potential for developing seaports to become major regional transshipment hubs [1].

Vietnam's current seaport system is systematically planned to be closely linked with major economic centers and regions nationwide. Large seaports are crucial hubs for import-export activities, contributing significantly to the entire region's economic growth. As a result, Vietnam's seaport infrastructure is well-positioned to leverage its strategic location and the growing demand for maritime transportation in the region. This infrastructure development enhances trade and strengthens Vietnam's role as a critical player in regional and global maritime commerce.

Some ports have been undergoing dredging upgrades to accommodate larger vessels and exploit domestic and international maritime services. In particular, the Nghi Son Economic Zone is developing industrial zones, increasing the volume of goods that need to be transported by both road and waterways, with water transportation accounting for 80–90% of the cargo volume. Water transportation reduces transportation costs and enhances investment efficiency for businesses while leveraging Thanh Hoa province's strengths with its extensive coastline [2].

According to the development plan of the Nghi Son port area, dredging and operation of berths 9 and 10 are scheduled for implementation in 2022 to accommodate vessels with a capacity of 100,000 DWT. The dredged volume of mud and sand in the port will be disposed of into the sea in offshore areas located 5 km away from the port [2].

Hydraulic models predict the spread of turbidity caused by dredging activities, allowing for a better understanding of how sediment plumes disperse in the marine environment. This information is crucial for evaluating potential impacts on water quality, marine ecosystems, and coastal habitats. Furthermore, hydraulic models can help design mitigation measures to minimize adverse environmental effects. For example, adjusting dredging methods or scheduling dredging activities during optimal tidal conditions may reduce the spread of sediment plumes and mitigate impacts on marine ecosystems.

Many studies have assessed the environmental impact of sand mining on coral reef ecosystems and seagrass beds through sedimentation [3–5]. Jones had been describing sediment particle sizes in the water column/ seabed, suspended sediment concentrations at different temporal scales during natural and dredging-related turbidity events, and changes in light quantity/quality underneath plumes. These conditions differ considerably from those used in past laboratory studies of the effects of sediments on corals [6]. The MIKE hydraulic model developed by the Danish Hydraulic Institute has been widely applied in studies simulating hydrodynamic regimes and environments, particularly using these toolsets to calculate the dispersion of pollutants from economic development activities such as dredging and dredge material disposal [7–13].

Overall, hydraulic models are essential for assessing the environmental impact of port upgrade projects, ensuring sustainable development, and minimizing adverse effects on the marine environment.

METERIAL AND METHODS

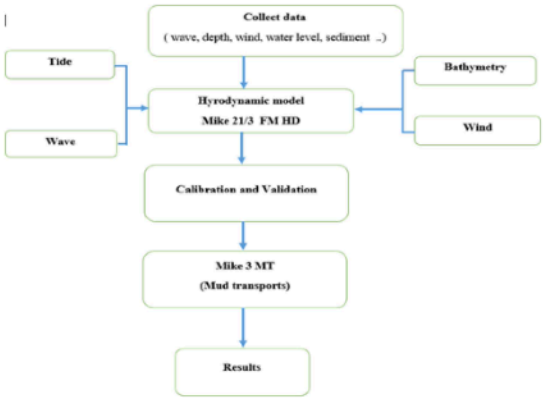

Figure 1. Study approach flowchart

This study used the Mike 3 model to simulate turbidity dispersion in the study area during the monsoon. The first stage of the simulation involves collecting data, including wave, wind, depth, and water level. Then, the model (calibration and validation) is set up using input data such as tide and monsoon. After simulated hydraulic, the result can be used for turbidity propagation simulations (Fig. 1).

The model is based on the solution of the three-dimensional incompressible Reynolds averaged Navier-Stokes equations, subject to Boussinesq and hydrostatic pressure assumptions. The local continuity equation is written as [13]:

$$\frac{\partial u}{\partial x}+\frac{\partial v}{\partial y}+\frac{\partial w}{\partial z}=S \quad (1)$$

And the two horizontal momentum equations for the *x*- and *y*- component, respectively.

$$\frac{\partial u}{\partial t}+\frac{\partial u^2}{\partial x}+\frac{\partial vu}{\partial y}+\frac{\partial wu}{\partial z}=fv-g\frac{\partial \eta}{\partial x}-\frac{1}{\rho_o}\frac{\partial p_a}{\partial x}-\frac{g}{\rho_o}\int_z^\eta \frac{\partial \rho}{\partial x}dz-\frac{1}{\rho_o h}\left(\frac{\partial s_{xx}}{\partial x}+\frac{\partial s_{xy}}{\partial y}\right)+F_u\frac{\partial}{\partial z}\left(v_t\frac{\partial u}{\partial z}\right)+u_s \quad (2)$$

$$\frac{\partial u}{\partial t}+\frac{\partial u^2}{\partial x}+\frac{\partial vu}{\partial y}+\frac{\partial wu}{\partial z}=fv-g\frac{\partial \eta}{\partial x}-\frac{1}{\rho_0}\frac{\partial p_a}{\partial x}-\frac{g}{\rho_0}\int_z^\eta \frac{\partial \rho}{\partial x}dz-\frac{1}{\rho_0 h}\left(\frac{\partial s_{xx}}{\partial x}+\frac{\partial s_{xy}}{\partial y}\right)+F_u\frac{\partial}{\partial z}\left(v_t\frac{\partial u}{\partial z}\right)+u_s \quad (3)$$

$$\frac{\partial v}{\partial t}+\frac{\partial v^2}{\partial y}+\frac{\partial uv}{\partial x}+\frac{\partial wv}{\partial z}=-fu-g\frac{\partial \eta}{\partial y}-\frac{1}{\rho_0}\frac{\partial p_a}{\partial y}-\frac{g}{\rho_0}\int_z^\eta \frac{\partial \rho}{\partial y}dz-\frac{1}{\rho_0 h}\left(\frac{\partial s_{yx}}{\partial x}+\frac{\partial s_{yy}}{\partial y}\right)+F_v\frac{\partial}{\partial z}\left(v_t\frac{\partial v}{\partial z}\right)+v_s s \quad (4)$$

where: t is the time; *x*, *y*, and *z* are the Cartesian co- ordinates; η is the surface elevation; *d* is the still water depth; h = η + *d* is the total water depth; *u*, *v*, and *w* are the velocity components in the *x*, *y*, and *z* direction; 2ΩsinΦ is the Coriolis parameter (Ω is the angular rate of revolution and Φ the geographic latitude); *g* is the gravitational acceleration; ρ is the density of water; s_{xx}, s_{xy}, s_{yx}, and s_{yy} are components of the radiation stress tensor; v_t is the vertical turbulent (or eddy) viscosity; p_a is the atmospheric pressure of the discharge due to point sources and (v_s, u_s) is the velocity by which the water is discharged into the ambient water [14].

Data of model

Bathymetry data in the shallow water were used using a bathymetry map with the rate of 1/5,000; observed from 2007 to 2015 by the Department of Survey, Mapping and Geographic Information, Ministry of Natural resources and Environment. In the offshore area, a rate bathymetry map of 1/50,000 was used from Global data [15].

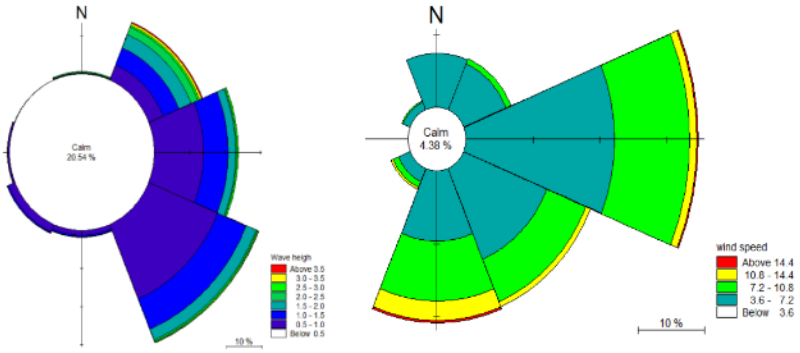

a) b)

Figure 2. Wave mapping at Hon Me station (a) and Win mapping at Sam Son station (b)

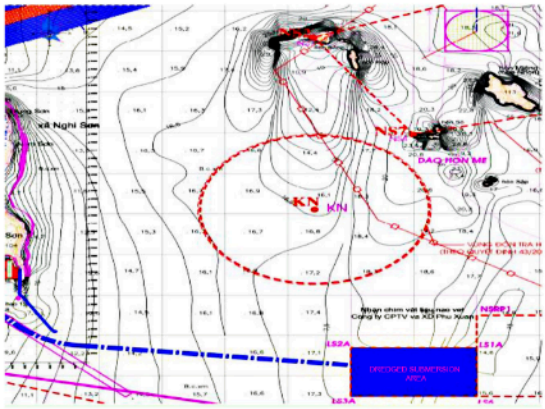

Figure 3. Sediment dumping area [2]

Hydrometeorological data serving the establishment models hydraulic model includes data series on water level, waves, currents, and winds in the study area. Wave data were collected by Hon Me station combined with Global wave data from January to December 2021, as shown in figure [9]. The study area is in the Gulf of Tonkin, influenced by the marine atmospheric system. This study used daily average wind data at Sam Son station in 2021 to serve the establishment of the hydraulic model as shown in the following Figures 2 and 3.

The actual water level measured in the study area is used in model evaluation by calibrating and verifying the hydraulic model. The study used a series of accurate data measured at Hon Me, Tinh Gia, and Thanh Hoa marine stations, with data collected in 2021.

Sediment data: The total volume of dredged material is divided mainly into mud and sand, with a ratio of 86:14 (based on the analysis results of mud samples in the dredging area). Mud is a spreading material, while sand is a settling material. The mud has a density of 1,050 kg/m^3, settling velocity of 0.015 m/s, and critical shear stress of 0.02 N/m^2 (primarily involved in dispersion), while sand has a density of 2,650 kg/m^3, settling velocity of 0.3 m/s, and critical shear stress of 0.5 N/m^2. The concentrations of mud and sand do not change during dredging trips. The total dredged volume is 2,804,700 m^3 and disposed of in the designated area [2].

The entire volume of dredged material in Nghi Son Port will be disposed of at the southern location of Hon Me Island. This area is 240 hectares delimited by control points (LA1A, LS2A, LS3A, LS6), with the seabed topography ranging from -15 m to -17.7 m (Table 1).

Table 1. Sediment dumping location [2]

Location	Longitude X (m)	Latitude Y (m)
LS1A	2,133,700	594,000
LS2A	213,700	592,000
LS3A	2,132,500	592,000
LS6	2,132,500	594,000

RESULTS AND DISCUSSION

Set up model

The computation grid in the study areas included all Thanh Hoa sea with a length of 45 km and a width of 30 km from the coastline. The resulting computation grid file in the Flow model was an ASCII file with an extension (mesh) that includes information on the geographical and water depth at node points in the mesh. The file also included information about the 6,549 nodes connectivity of the 12,173 triangular elements (Fig. 4).

Calibration and validation model: Calibration simulation has been acted by changing bed resistance with a value given as a Manning number of 30; 32, 35 m$^{1/3}$/s. The new finite-volume model has been successfully tested in several basic, idealized simulations for which computer results can be compared with analytical solutions. This study used the Nash coefficient for the calibration and validation model.

$$Nash = 1 - \frac{\sum \left(Xo,i - Xs,i \right)^2}{\sum \left(Xo,i - \overline{Xo} \right)^2}$$

where: Xo,i: observed value; Xs,i: computer value; $\overline{Xo}$: average observed value.

The research has used observer water level and wave heigh value in Hon Me station (19°22': 105°57') during 2021 January for calibration and July for validation. The result of the comparison between observation and computer water level showed in the Figures 5 and 6.

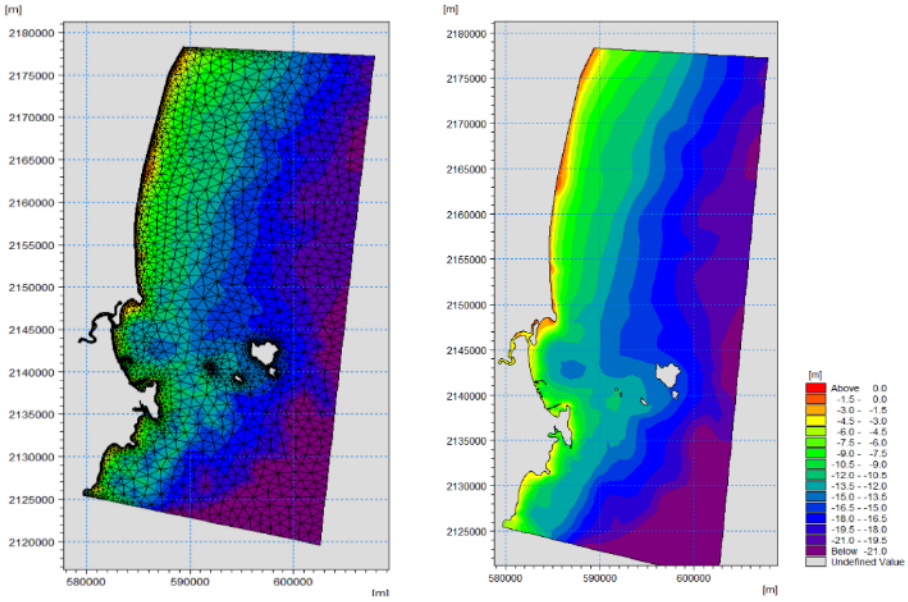

Figure 4. Computation grid of study area

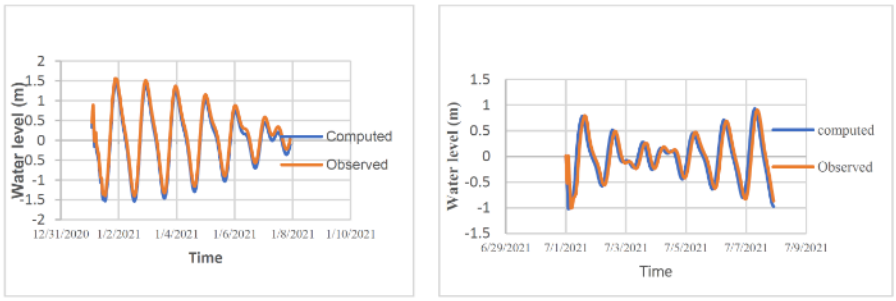

a) b)

Figure 5. Comparing water level observed and computed in calibration(a) and validation (b)

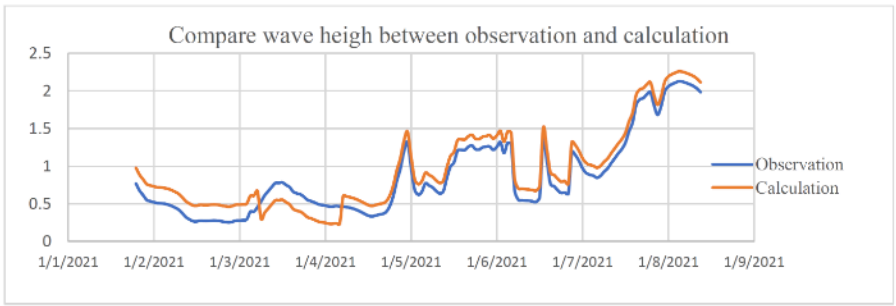

Figure 6. Validation wave heigh in the study areas

Table 2. Nash coefficients in calibration, validation

No.	Set up model	Nash
1	Calibration	0.92
2	Validation	0.86

The result shows that the water level line computed and observed is the same shape with high Nash coefficients from 0.83 to 0.92 (Table 2). The calibration and validation model process has been successful for the study area

so that the research can be an application model for oil spill simulation.

Result of hydraulic simulation in the Northeast monsoon period

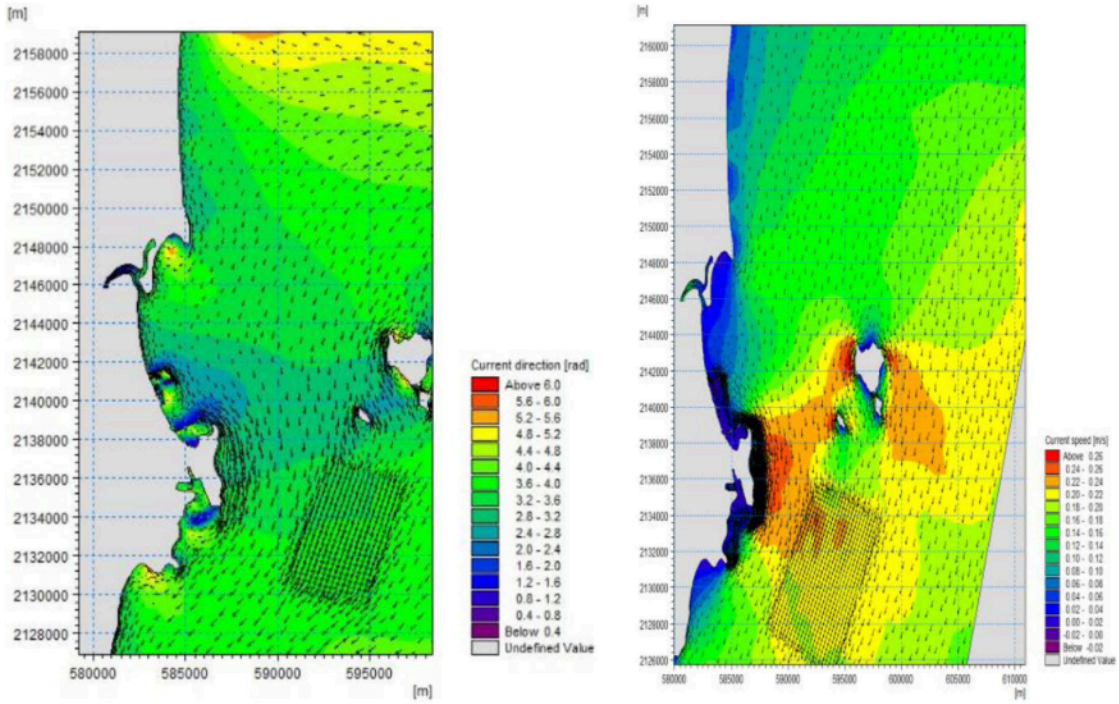

a) b)

Figure 7. Current direction (a) and current speed of area study (b)

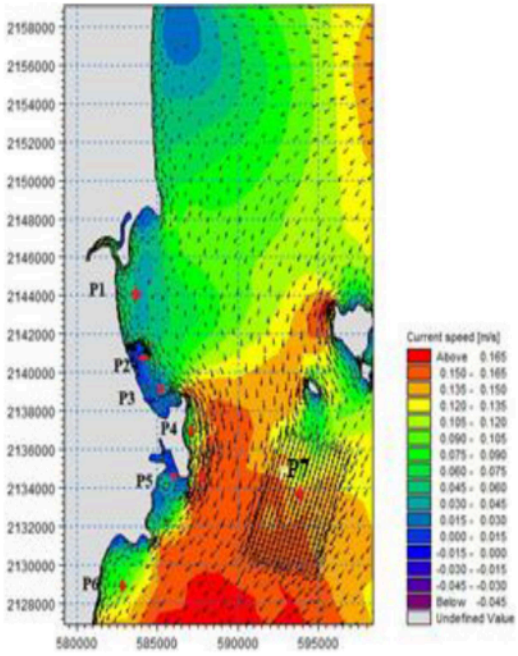

Figure 8. Checking location of current speed

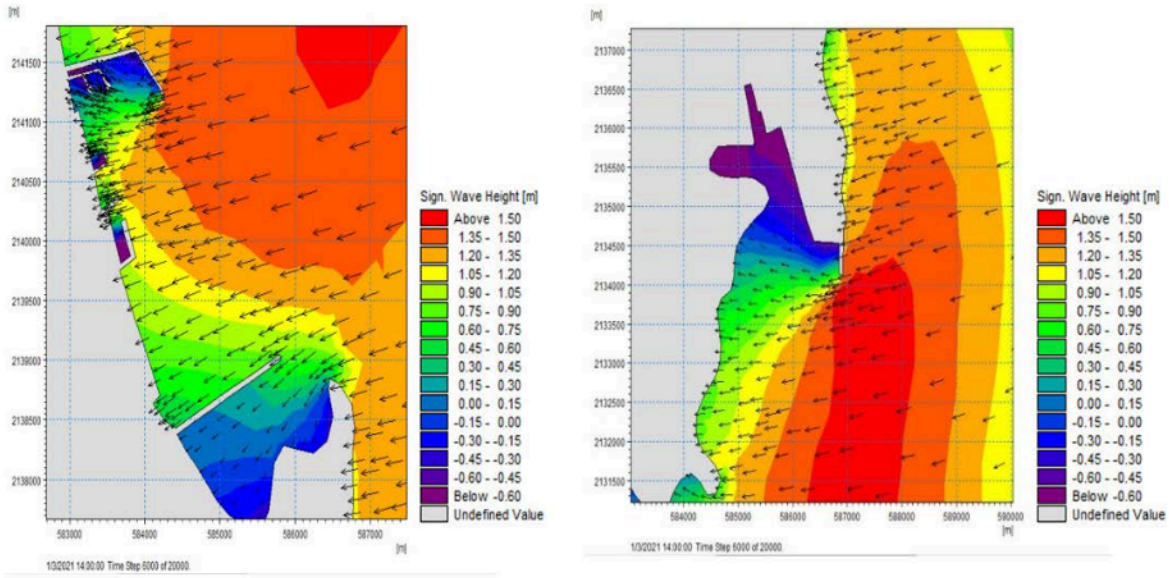

Figure 9. Wave high in the North (a) and South of Nghi Son harbor (b)

The simulation result for the Northeast monsoon shows that the current direction of the shore in the area study was North-South. In contrast, current speed significantly decrease in the harbor due to being shielded by Nghi Son Island and the dike sea (Figs. 7–9).

As shown in Table 2, the current speed in the checking illustrated average current speed inshore area stands at about 0.06 m/s to 0.09 m/s at the P_1 and P_2, respectively. In comparison, due to coastal morphology, P_4 location had current speed 0.12 m/s, which was a higher than that of P_1 and P_6. The P_2, P_3, and P_5, located inside Nghi Son harbor, had a significant low current speed of 0.03 m/s to 0.04 m/s, whereas the P_7 point had the largest average current speed of 0.15 m/s.

The simulation results shows that waves high in Hon Me island's inside harbor and southwest coastline had values from 0.2 m to 0.6 m, while that of the P7 station accounted 0.8 m. In the south of Nghi Son harbor, the barrier island combined with the sea dike had a small average wave high with a value of 0.2 m (Table 3).

Table 3. Current speed in the study area

Location	P_1	P_2	P_3	P_4	P_5	P_6	P_7
Maximum of current speed (m/s)	0.86	0.60	0.61	1.15	0.76	1.02	1.49
Average of current speed (m/s)	0.06	0.03	0.03	0.12	0.04	0.09	0.15

Result of hydraulic simulation in the Southwest monsoon

The average current speed at the test locations showed that the maximum speed occurs at positions P7 and P4 with a value of 0.16 m/s, while the coastal current in the study area had a value only from 0.03 m/s to 0.09 m/s (Tables 4, 5).

Generally, the average wave height value at the test sites during the northeast monsoon was more prominent than in the Southwest. At

point P_7, the average wave height reached 1.3 m in the Southwest monsoon, which was higher than that of the Northeast monsoon period, with 0.81 m (Table 6, Figs. 10 and 11).

Table 4. Current speed of points in the study area

Location	P_1	P_2	P_3	P_4	P_5	P_6	P_7
Maximum of current speed (m/s)	0.13	0.21	0.18	0.49	0.14	0.17	0.30
Average of current speed (m/s)	0.09	0.03	0.03	0.16	0.05	0.09	0.16

Table 5. Table comparing current speed in periods

Location	P_1	P_2	P_3	P_4	P_5	P_6	P_7
Average of current speed in Southwest monsoon period (m/s)	0.09	0.03	0.03	0.16	0.05	0.09	0.16
Average of current speed in Northeast monsoon period (m/s)	0.06	0.03	0.03	0.12	0.04	0.09	0.15

Table 6. Wave height comparison

Location	P_1	P_2	P_3	P_4	P_5	P_6	P_7
Average of wave high in Southwest monsoon periods (m/s)	0.35	0.28	0.12	0.51	0.64	0.60	0.81
Average of wave high in Northeast monsoon periods (m/s)	0.91	0.24	1.03	1.16	0.12	0.63	1.30

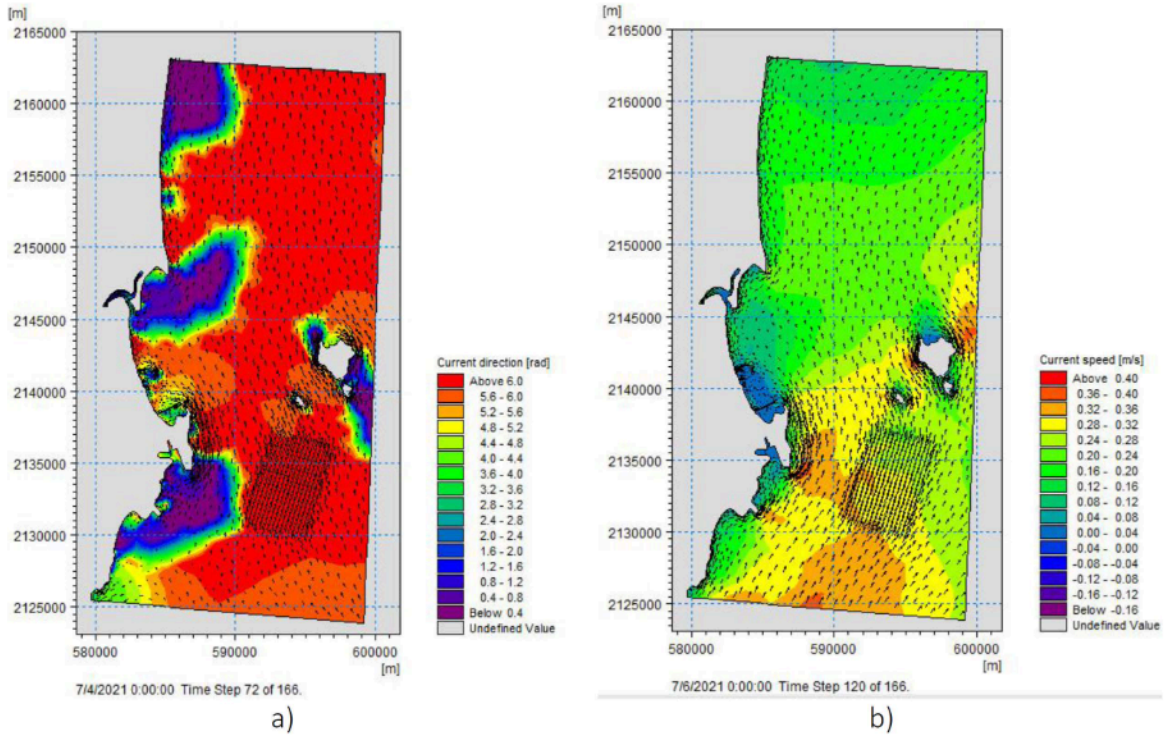

Figure 10. Current directions (a) and current speed in the Southwest monsoon(b)

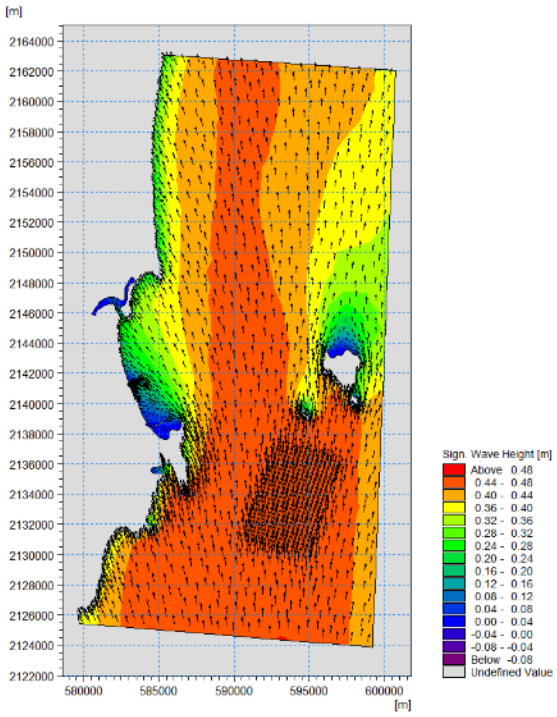

Figure 11. Wave high in Nghi Son harbor in the Southwest monsoon period

Result of simulation turbidity dispersion during the Northeast monsoon period

The research utilized the Mike 3 model to calculate the turbidity propagation during the sediment mud deposition process in the study area. The results of turbidity propagation are illustrated in the following Figure 12.

From the simulation results of turbidity after 4 weeks of sediment mud deposition, the highest sediment mud concentration reached a value of 0.052 kg/m^3 with a radius of approximately 200 m around the deposition point. The area surrounding the deposition point with a radius of 700 m had sediment mud concentrations ranging from 0.024 kg/m^3 to 0.048 kg/m^3. After 6 weeks of construction, the turbidity field reached a value of 0.09 kg/m^3 with an influence radius of 250 m. Meanwhile, within a radius of 2.5 km, the sediment mud concentration reached a value of 0.036 kg/m^3.

After 8 weeks of construction, the sediment mud concentration field with an influence radius of approximately 3.5 km ranged from 0.045 kg/m^3 to 0.135 kg/m^3. The highest sediment mud concentration reached a value of 0.135 kg/m^3, corresponding to an influence radius of approximately 0.5 km.

After 10 weeks of construction, the sediment mud deposition in the research area indicated a gradual increase in concentration, with the highest turbidity reaching a value of 0.18 kg/m^3 and an influence radius of approximately 0.7 km. The area affected by the turbidity field ranged from 0.015 kg/m^3 to 0.18 kg/m^3 up to a radius of 2.2 km.

After 12 weeks of construction, the influence radius of the sediment mud concentration field is approximately 1.5 km, with sediment mud concentrations ranging from 0.04 kg/m^3 to 0.2 kg/m^3. Within this radius, the area with the greatest sediment mud concentration, approximately 0.2 kg/m^3, is found within a radius of about 0.5 km. After 14 weeks, the influence radius due to the sediment mud concentration extends to about 2.5 km, with sediment mud concentrations ranging from 0.003 kg/m^3 to 0.13 kg/m^3.

After 16 weeks of sediment mud deposition in the research area, the sediment mud concentration ranges from 0.016 kg/m^3 to 0.104 kg/m^3, with an influence radius of approximately 1.8 km. Within this range, the highest sediment mud concentration reaches 0.104 kg/m^3, with a radius of approximately 0.5 km.

After 18 weeks of construction, the influence radius of the sediment mud concentration field is about 1.5 km. The concentrations range from 0.02 kg/m^3 to 0.14 kg/m^3. Within this range, the area with the highest sediment mud concentration, reaching 0.14 kg/m^3, has an influence radius of 0.75 km.

After 20 weeks of sediment mud deposition in the research area, there is a significant increase in sediment mud concentration, with the highest value reaching 0.4 kg/m^3. The influence radius of the sediment mud concentration with this value (0.4 kg/m^3) is 0.25 km, indicating where this concentration is predominant. Additionally, the influence radius of the sediment mud concentration with a value of 0.2 kg/m^3 is 0.9 km. Furthermore, the area affected by the sediment mud concentration up to a value of 0.04 kg/m^3 has an influence radius of 2 km.

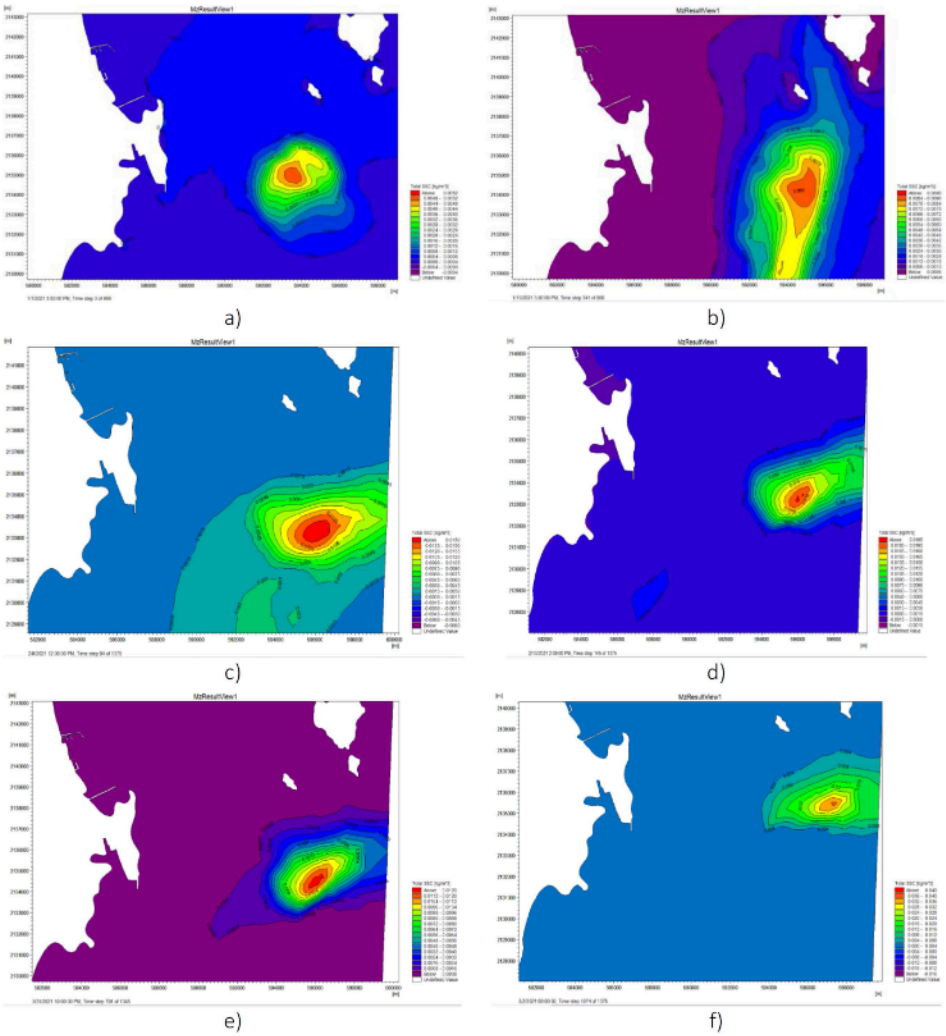

Figure 12. The propagation of turbidity during the sediment mud deposition process. (a) The scope of influence of sediment mud concentration after 4 weeks; b) The scope of influence of sediment mud concentration after 6 weeks; c)The scope of influence of sediment mud concentration after 8 weeks; d) The scope of influence of sediment mud concentration after 10 weeks; e) The scope of influence of sediment mud concentration after 16 weeks; f) The scope of influence of sediment mud concentration after 20 weeks

Result of simulation turbidity dispersion during the Southwest monsoon period

The calculation of turbidity propagation from sediment mud deposition in the research area is based on the combined use of the Hydraulic Module (HD) under Southwest monsoon conditions and the Sediment Transport Module (MT) (Fig. 13).

The simulation results of sediment mud deposition in the research area show that during the Southwest monsoon period, the direction of sediment mud turbidity movement tends to be closer to the coastal and Hon Me Island areas than during the Northeast monsoon period.

The extent of the influence radius of sediment mud concentration exceeding the threshold during the sediment mud deposition process is approximately 0.7 km. However, it is noted that the coastal area and near Hon Me island has sediment mud concentration levels

within the permissible threshold for turbidity standards set by the Ministry of Natural Resources and Environment (according to QCVN 10-MT:2015/BTNMT).

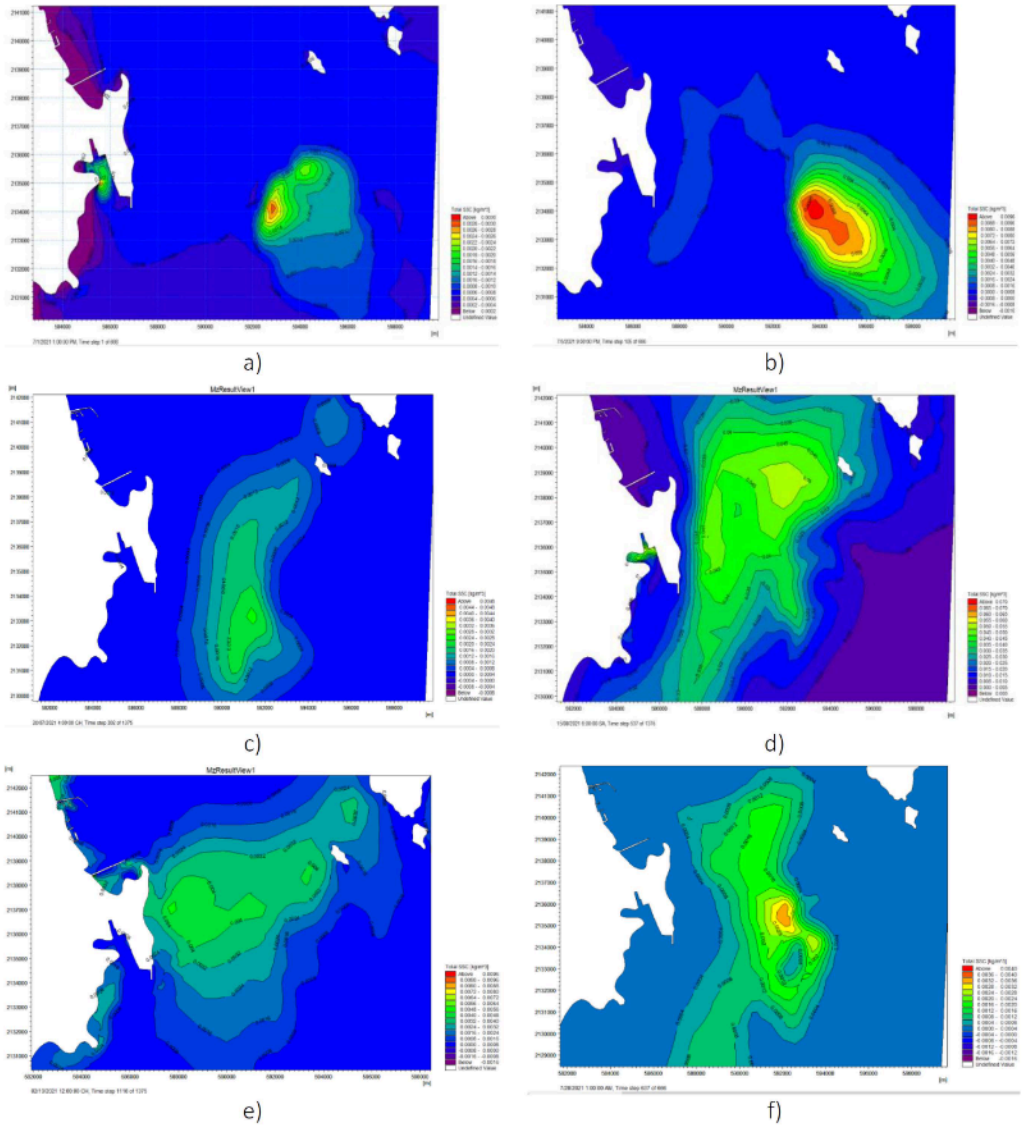

*Figure 13.*The propagation of turbidity during the southwest monsoon period. (a) The scope of influence of sediment mud concentration after 4 weeks; b) The scope of influence of sediment mud concentration after 6 weeks; c)The scope of influence of sediment mud concentration after 8 weeks; d) The scope of influence of sediment mud concentration after 10 weeks; e) The scope of influence of sediment mud concentration after 16 weeks; f) The scope of influence of sediment mud concentration after 20 weeks

The following figures show the simulation results for two perpendicular cross-sections of the submerged area, which assess the turbidity field with depth in the submerged research area (Figs. 14 and 15).

The calculation results of sediment mud concentration at cross-section 2 along the sediment deposition line in the research area are depicted in the following Figure 16.

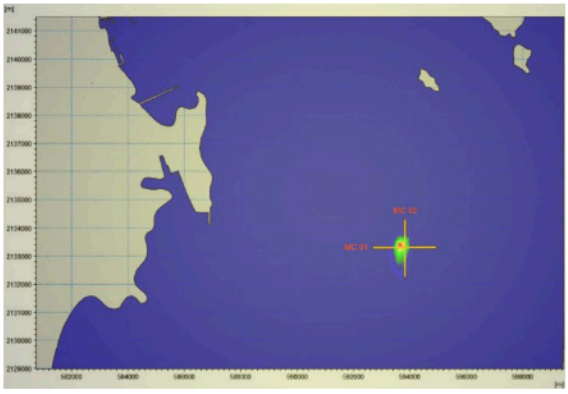

Figure 14. The cross-section examines the sediment mud concentration field with depth

The calculated sediment mud concentration results with depth at the sediment deposition site in the research area show that the sediment mud concentration ranges from 0.01–0.4 kg/m^3, distributed in the seabed area at depths from -14 m to -18 m. The sediment mud concentration tends to decrease towards the water surface. The sediment mud concentration is relatively low in the upper water layer, from 0.01–0.08 kg/m^3, with depths ranging from 0 to -5 m.

Through the analysis of cross-sections along two parallel lines, it was observed that along the line from offshore to the shore, the turbidity plume exceeding 0.04 kg/m^3 has a maximum length of 4–5 km after 20 weeks of sediment deposition.

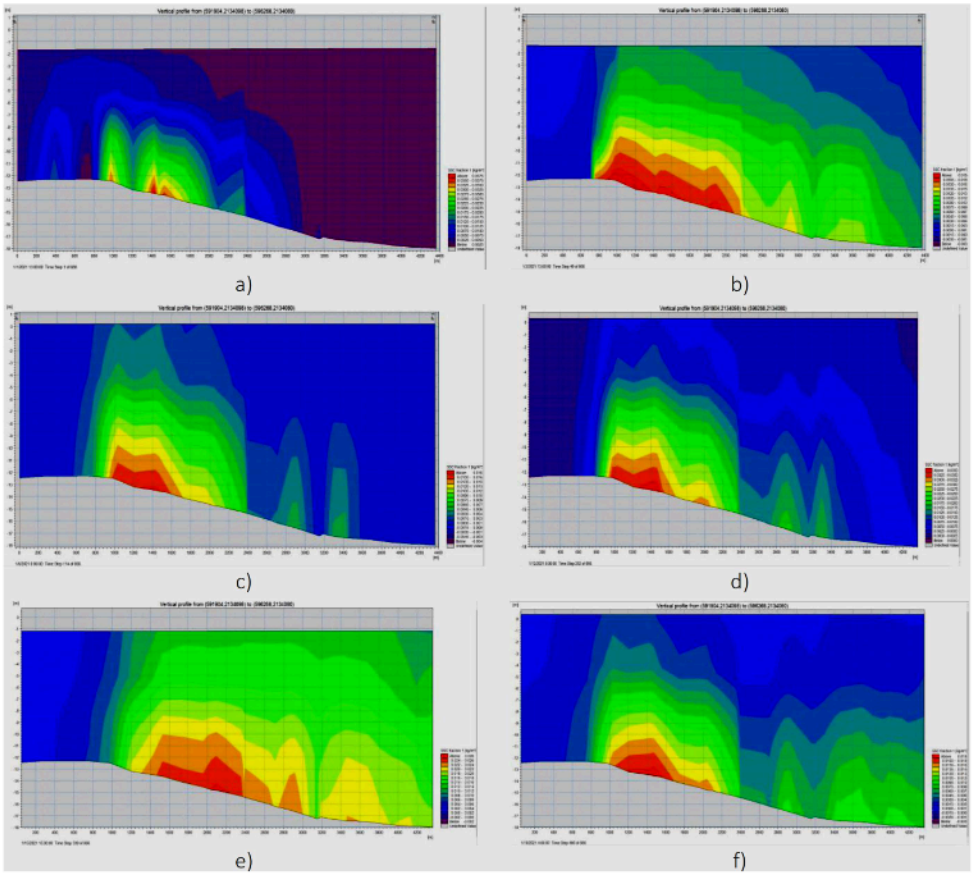

Figure 15. The distribution of sediment mud concentration with depth at cross-section MC01. (a)The sediment mud concentration field with depth after 4 weeks; b) The sediment mud concentration field with depth after 6 weeks; c) The sediment mud concentration field with depth after 8 weeks; d) The sediment mud concentration field with depth after 10 weeks; e) The sediment mud concentration field with depth after 16 weeks; f) The sediment mud concentration field with depth after 20 weeks

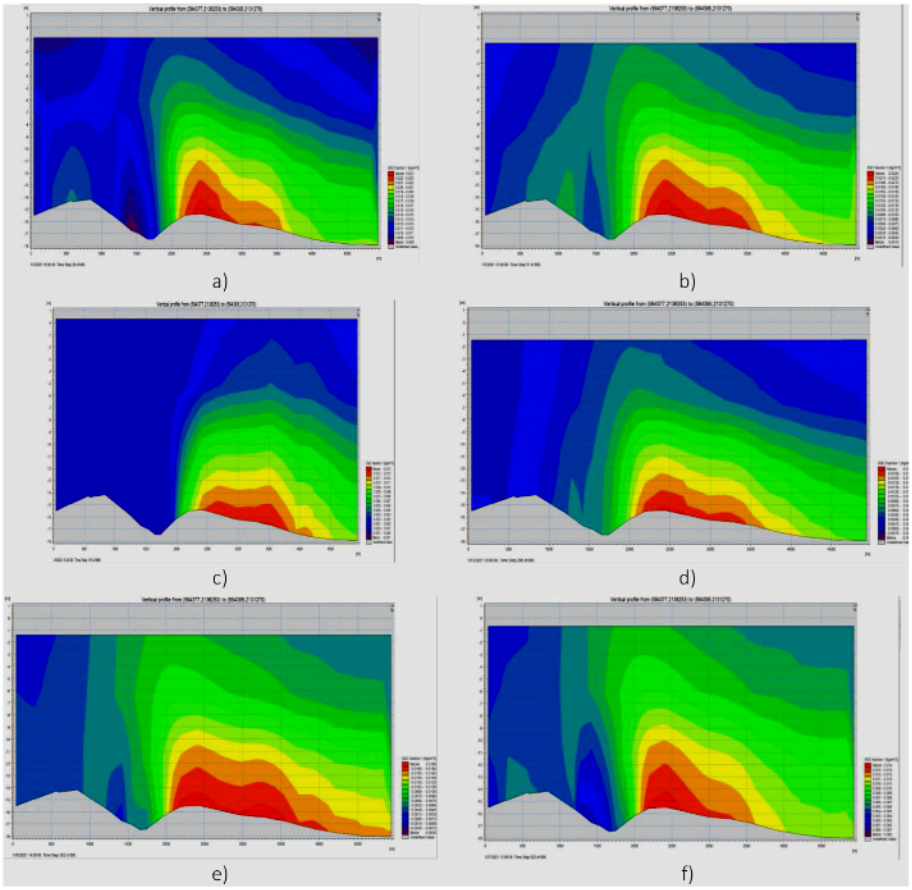

Figure 16. The distribution of sediment mud concentration with depth at cross-section MC02 (a)The sediment mud concentration field with depth after 4 weeks; b) The sediment mud concentration field with depth after 6 weeks; c) The sediment mud concentration field with depth after 8 weeks; d) The sediment mud concentration field with depth after 10 weeks; e) The sediment mud concentration field with depth after 16 weeks; f) The sediment mud concentration field with depth after 20 weeks

CONCLUSION

The research has successfully applied a Mike 3 hydraulic model to compute the hydrodynamic regime in the research area under Northeast and Southwest monsoon conditions. This model aids in constructing input datasets for calculating turbidity propagation from sediment mud deposition activities in the Nghi Son sea area, Thanh Hoa Province.

The dispersion process of turbidity concentration during sediment deposition is greatly influenced by the hydrodynamic regimes during the monsoon seasons. During the Northeast monsoon period, the sediment mud concentration field is distributed southward from the deposition area, with sediment mud concentrations ranging from 0.01–0.4 kg/m^3 within an influence radius of approximately 2.5 km.

During the southwest monsoon period, the turbidity concentration distribution expands northward from the deposition area due to the influence of wind and currents during this season. The northern area of Nghi Son port is affected by the dispersion of turbidity concentrations below 0.04 kg/m^3. The area surrounding Hon Me island has sediment mud concentrations ranging from 0.015–0.025 kg/m^3.

The turbidity concentration distribution with depth ranges from 0.01 kg/m^3 to 0.4 kg/m^3 and is primarily located at the seafloor depths ranging from -14 m to -18 m. The turbidity concentration gradually decreases towards the water surface. The turbidity concentration is relatively low in the upper water layer, from 0.01–0.08 kg/m^3, with depths ranging from 0 to -5 m, Along the offshore-to-shore cross-section, concentrations exceeding 0.04 kg/m^3 have a maximum length of 4–5 km after 20 weeks of sediment deposition.

In the recent study, only the adjustment and validation of the hydraulic model parameters were accomplished without addressing environmental factors. Therefore, additional environmental data collection is necessary in the research area to facilitate model calibration and enhance the accuracy of research findings.

REFERENCES

[1] Journal on Information and Communications, 2022. https://ictviet-nam.vn/tiem-nang-phat-trien-cua-nganh-hang-hai-viet-nam-53779.html; accessed January 20, 2024 (in Vietnamese).

[2] People's Committee of Thanh Hoa Province, 2024. https://thanhhoa.gov.vn; accessed January 25, 2024 (in Vietnamese).

[3] Erftemeijer, P. L., and Lewis III, R. R. R., 2006. Environmental impacts of dredging on seagrasses: a review. *Marine pollution bulletin*, *52*(12), 1553–1572. doi: 10.1016/j.marpolbul.2006.09.006

[4] Erftemeijer, P. L., Riegl, B., Hoeksema, B. W., and Todd, P. A., 2012. Environmental impacts of dredging and other sediment disturbances on corals: a review. *Marine pollution bulletin*, *64*(9), 1737–1765. doi: 10.1016/j.marpolbul.2012.05.008

[5] Erftemeijer, P. L. A., 2006. Managing the effects of dredging on seagrass in the Mediterranean Sea. *Biologia marina mediterranea*, *13*(4), 183–188.

[6] Jones, R., Bessell-Browne, P., Fisher, R., Klonowski, W., and Slivkoff, M., 2016. Assessing the impacts of sediments from dredging on corals. *Marine Pollution Bulletin*, *102*(1), 9–29. https://doi.org/10.1016/j.marpolbul.2015.10.049

[7] Quang Tri, D., Kandasamy, J., and Cao Don, N., 2019. Quantitative assessment of the environmental impacts of dredging and dumping activities at sea. *Applied Sciences*, *9*(8), 1703. https://doi.org/10.3390/app9081703

[8] National Oceanic and Atmospheric Administration, 2024. https://www.ncei.noaa.gov/maps-and-geospatial-products; accessed January 25, 2024.

[9] Lan, V. V., Lan, N. H., Mai, N. T., and Nga, V. T. T., 2024. Study on the influence of monsoon regimes on the spread of turbidity from dredging activities at Nghi Son Port, Thanh Hoa Province. *Journal of Natural Resources and Environment Science*, 50, 1–17. (in Vietnamese).

[10] Van Maren, D. S., van Kessel, T., Cronin, K., and Sittoni, L., 2015. The impact of channel deepening and dredging on estuarine sediment concentration. *Continental Shelf Research*, *95*, 1–14. https://doi.org/10.1016/j.csr.2014.12.010

[11] Davies, S., Mirfenderesk, H., Tomlinson, R., and Szylkarski, S., 2009. Hydrodynamic, water quality and sediment transport modeling of estuarine and coastal waters on the gold coast Australia. *Journal of Coastal Research*, 937–941.

[12] Menendez, A. N., Badano, N. D., Lopolito, M. F., and Re, M., 2013. Water quality assessment for a coastal zone through numerical modeling. *Journal of Applied Water Engineering and Research*, *1*(1), 8–16. doi: 10.1080/23249676.2013.827892

[13] DHI, 2011. MIKE 3. Hydrodynamic Module. User Guide. https://www.man-ualslib.com/manual/2974729/Dhi-Mike-3-Flow-Model-Fm.html; accessed January 25, 2024.

[14] DHI, 2011. MIKE 21/3. Mud transport Model. User Guide. https://www.dhi-group.com/technologies/mikepoweredby dhi/mike-21-3-mud-transport; accessed January 25, 2024

[15] National Oceanic and Atmospheric Administration, 2024. https://coastwatch.pfeg.noaa.gov; accessed January 25, 2024.